
Generation of gravitational waves during inflation

A project report
submitted in partial fulfilment for the award of the degree of
B.S & M.S in Physics
by
Poruri Sai Rahul
under the guidance of
Dr. L. Sriramkumar



Department of Physics
Indian Institute of Technology Madras
Chennai 600036, India
June 2015

CERTIFICATE

This is to certify that the project titled **Generation of gravitational waves during inflation** is a bona fide record of work done by **Poruri Sai Rahul** towards the partial fulfilment of the requirements of the B.S & M.S degree in Physics at the Indian Institute of Technology, Madras, Chennai 600036, India.

(L. Sriramkumar, Project supervisor)

ACKNOWLEDGEMENTS

I cannot express in words my gratitude to **Dr. L. Sriramkumar** for guiding me, regarding my work and my personal life. I would also like to thank V. Sreenath and Debika Choudhury for helping me with my project and for clarifying my doubts. I would like to thank my family and my friends, especially Shashi Kunwar and Preeti Saryan, who have kept me on my toes over the last few years.

ABSTRACT

We are currently in an era of precision cosmology. The precision with which anisotropies in the Cosmic Microwave Background, CMB for short, are being measured has increased tremendously over the years, thanks to the efforts of the Planck and the WMAP missions. The theory of inflation predicts the presence of such anisotropies. In this work, I study the generation and evolution of tensor perturbations, otherwise referred to as gravitational waves, during inflation. The aim of this project is to construct a python code to numerically evaluate the tensor power spectrum for two different models of inflation, namely power law inflation and inflation driven by a small field model of potential.

Contents

1	Introduction	1
1.1	Conventions and notations	1
1.2	Driving inflation	2
1.3	Metric perturbations	3
1.4	Quantization of perturbations	5
2	Inflationary models	7
2.1	Power law inflation	8
2.1.1	The Bunch-Davies initial conditions	10
2.1.2	Tensor power spectrum	10
2.2	Inflation driven by small field potential	11
3	Numerical results	12
3.1	Power-law inflation	12
3.2	Inflation driven by a small field potential	15
4	Summary	19
	Appendix A Python Code	22

List of Figures

3.1	Plot of $\phi(N)$ as a function of N during power law inflation	13
3.2	Plot of $H(N)$ as a function of N during power law inflation	14
3.3	Plot of $\epsilon_1(N)$ as a function of N during power law inflation	14
3.4	Plot of $\mathcal{P}_T(k)$ as a function of k during power law inflation	16
3.5	Plot of $\phi(N)$ as a function of N during inflation driven by a small field potential	16
3.6	Plot of $H(N)$ as a function of N during inflation driven by a small field potential	17
3.7	Plot of $\epsilon_1(N)$ as a function of N during inflation driven by a small field potential	17
3.8	Plot of $\mathcal{P}_T(k)$ as a function of k during inflation driven by a small field potential	18

Chapter 1

Introduction

Inflation refers to a period of rapid expansion during the early stages of the radiation dominated epoch of our universe. Inflation solves two of the biggest drawbacks of the Hot big bang model namely the horizon problem and the flatness problem. (For a detailed review of the horizon problem see Ref. [1].)

This work presents a study of the generation and evolution of tensor perturbations and the power spectrum of tensor perturbations generated during two models of inflation, namely power law inflation and inflation driven by a small field potential model. In this chapter, I shall describe the need for scalar fields and the conditions imposed upon them to drive inflation. I shall briefly discuss linear perturbation theory and discuss tensor perturbations in the metric. In the next chapter, I shall outline how given a form of the scale factor $a(t)$ we can arrive at the dependence of the scalar field ϕ and the potential $V(\phi)$ with respect to cosmic time t . After solving the background equations, I shall discuss the solution to the equation governing tensor perturbations and the power spectrum of the tensor perturbations. Finally, I shall discuss the numerical solutions we obtained for the power spectrum of tensor perturbations for the two aforementioned models of inflation.

1.1 Conventions and notations

Before we go any further, I shall list the conventions and notations adopted in this work. I shall work in $(3+1)$ - dimensions and I shall adopt the metric signature $(+, -, -, -)$. Greek indices denote all spacetime coordinates where as Latin indices, other than k , refer

to spatial coordinates. I define the Planck mass as $M_{\text{Pl}} = (8\pi G)^{-1/2}$ and for convenience, we shall work in units of $M_{\text{Pl}} = 1$. Cosmic time is denoted as t and an overdot denotes differentiation with respect to cosmic time where as the conformal time is denoted as η and an overprime denotes differentiation with respect to conformal time. The duration of inflation can also be measured in terms of number of e-folds N where N is defined as

$$N = \ln \left(\frac{a(t)}{a_0} \right), \quad (1.1)$$

where a_0 is the scale factor when inflation started and $a(t)$ is the scale factor when inflation ends.

1.2 Driving inflation

In order to achieve inflation and solve the horizon problem, it is necessary that

$$\ddot{a} > 0. \quad (1.2)$$

In a spatially flat, smooth, Friedmann universe, the line element is described by

$$ds^2 = dt^2 - a^2(t)d\mathbf{x}^2 = a^2(\eta) (d\eta^2 - d\mathbf{x}^2), \quad (1.3)$$

and for such a line element, the Einstein's equations can be rewritten as the following two Friedmann equations

$$\left(\frac{\dot{a}}{a} \right)^2 = H^2 = \left(\frac{8\pi G}{3} \right) \rho, \quad (1.4)$$

$$\left(\frac{\ddot{a}}{a} \right) = \dot{H} + H^2 = - \left(\frac{4\pi G}{3} \right) (\rho + 3p), \quad (1.5)$$

where ρ and p denote the energy density and pressure of the field driving the expansion and $H = \dot{a}/a$ is the Hubble parameter

From Eqs. (1.2) and (1.5), it is straight forward to see that

$$(\rho + 3p) < 0, \quad (1.6)$$

is a necessary condition for the field that drives inflation. We can check that neither matter, for which $p = 0$, nor radiation, for which $p = \rho/3$, satisfies the necessary condition. We can therefore, under the necessary conditions, invoke a generic scalar field ϕ and a corresponding potential $V(\phi)$ to drive inflation. A scalar field that drives inflation is also referred to as an Inflaton.

We can write the action for such a scalar field as

$$S[\phi] = \int d^4x \sqrt{-g} \left[\left(\frac{1}{2} \right) (\partial^\lambda \phi \partial_\lambda \phi) - V(\phi) \right], \quad (1.7)$$

and the stress-energy tensor for the corresponding scalar field is given by

$$T^\mu_\nu = \partial^\mu \phi \partial_\nu \phi - \delta^\mu_\nu \left[\left(\frac{1}{2} \right) (\partial^\lambda \phi \partial_\lambda \phi) - V(\phi) \right], \quad (1.8)$$

From Eqn. (1.7), we can derive the equations of motion for the scalar field as

$$\ddot{\phi} + 3H\dot{\phi} + V_\phi = 0, \quad (1.9)$$

where $V_\phi = dV/d\phi$.

1.3 Metric perturbations

Anisotropies in the CMB are one part in 10^5 and it can be inferred that they should be much smaller at earlier epochs given the expanding nature of our universe. We can therefore study the generation and evolution of such perturbations using linear perturbation theory.

According to their behaviour under local rotation of the spatial coordinates on hypersurfaces of constant time, the perturbations in a Friedmann background can be classified as scalars, vectors and tensors. Scalar perturbations remain invariant under rotations. In fact, scalar perturbations are what are most responsible for the anisotropy we see in our universe. Under local rotations, vector and tensor perturbations behave as vectors and tensors respectively. Rotational velocity fields generate the vector perturbations and are, therefore, also referred to as vorticity modes. Finally, gravitational waves are described by tensor perturbations. (For a discussion of cosmological linear perturbations theory, refer to Refs.

[1, 2, 3, 4, 5, 6, 7, 8, 9, 10].) For the scope of this work, I shall restrict myself to tensor perturbations of the metric.

The Friedmann line element describes a homogeneous and isotropic universe, which is not a valid assumption under the presence of perturbations. We can therefore choose to work in a variety of coordinate systems under the condition that they reduce to the standard Friedmann line element in the limit when the perturbations vanish. A gauge refers to a particular choice of coordinates and a gauge transformation refers to the transformation from one gauge to another. Therefore, we can choose to study the evolution of perturbations in terms of gauge-invariant quantities or work in a specific gauge throughout. We shall adopt the latter approach. As such, the tensor perturbations in the metric can be represented as

$$ds^2 = dt^2 - a^2(t)(\delta_{ij} + h_{ij})dx^i dx^j, \quad (1.10)$$

where the tensor perturbations are characterized by a transverse, traceless matrix h_{ij} .

In a similar fashion, we shall classify the sources of said metric perturbations, namely the stress-energy tensor. The stress energy tensor, similar to the metric tensor, is a symmetric two tensor. Therefore, perturbations in the stress-energy tensor can also be classified as scalar, vector and tensor components. A scalar field driving inflation, the inflaton, is a scalar source. Velocity fields with vorticity are vector sources. Having eliminated the scalar and vector contributions, anisotropic stresses constitute a tensor source. This is referred to as the decomposition theorem.

The perturbed Einstein tensors can be derived from the perturbed metric $\delta g_{\mu\nu}$. The Einstein's equations can then relate the perturbed Einstein tensors to the perturbed stress-energy tensor, say, $\delta T_{\mu\nu}$. These equations govern the evolution of metric perturbations. The decomposition theorem stated above dictates that the scalar, vector and tensor perturbations decouple and can therefore be studied independent of one another. In other words, scalar sources lead to scalar perturbations, vector sources lead to vector perturbations and tensor sources lead to tensor perturbations.

Under these assumptions, the perturbed Einstein tensors corresponding to the metric described by Eqn. (1.10) are given by

$$\delta G_0^0 = \delta G_i^0 = 0, \quad (1.11)$$

$$\delta G_j^i = - \left(\frac{1}{2} \right) \left(\ddot{h}_{ij} + 3H\dot{h}_{ij} - \frac{1}{a^2} \nabla^2 h_{ij} \right), \quad (1.12)$$

after imposing the conditions that h_{ij} is a transverse and traceless matrix.

Similarly, we can write the perturbed stress-energy tensor as

$$\delta T_0^0 = \delta \rho, \quad (1.13)$$

$$\delta T_i^0 = (\nabla_i \delta \sigma), \quad (1.14)$$

$$\delta T_j^i = -\delta p \delta_j^i. \quad (1.15)$$

In the absence of anisotropic stresses i.e if $\delta T_j^i = 0$, we get that

$$\ddot{h} + 3H\dot{h} - \left(\frac{1}{a^2} \right) \nabla^2 h = 0. \quad (1.16)$$

Eqn. (1.16) can be rewritten in terms of conformal time η as

$$h'' + 2\mathcal{H}h' - \nabla^2 h = 0, \quad (1.17)$$

where $\mathcal{H} = a'/a$.

1.4 Quantization of perturbations

In Fourier space, Eqn. (1.17) becomes

$$h_k'' + 2\mathcal{H}h_k' + k^2 h_k = 0. \quad (1.18)$$

The homogeneity of the Friedmann background allows us to quantize the tensor perturbations. Upon quantization, we can write the tensor perturbations \hat{h} in terms of its Fourier modes $h_k(\eta)$ as

$$\hat{h}(\eta, \mathbf{x}) = \int \frac{d^3\mathbf{k}}{(2\pi)^{3/2}} [\hat{a}_k h_k(\eta) e^{i\mathbf{k}\cdot\mathbf{x}} + \hat{a}_k^\dagger h_k^*(\eta) e^{-i\mathbf{k}\cdot\mathbf{x}}], \quad (1.19)$$

where the creation and annihilation operators, \hat{a}_k and \hat{a}_k^\dagger , follow the standard commutation relations. At the linear order in perturbations that we are working in, the power spectrum of the tensor perturbations can be characterized by the two point function of the quantum field \hat{h} . The power spectrum of the tensor perturbations $\mathcal{P}_T(k)$ and the two point function are related by

$$\int_0^\infty dk \mathcal{P}_T(k) = \int d^3\mathbf{k} \int \frac{d^3(\mathbf{x} - \mathbf{x}')}{(2\pi)^3} \langle 0 | \hat{h}(\eta, \mathbf{x}) \hat{h}(\eta, \mathbf{x}') | 0 \rangle e^{-i[\mathbf{k}\cdot(\mathbf{x}-\mathbf{x}')]}, \quad (1.20)$$

where $|0\rangle$ is the vacuum state defined as $\hat{a}_k|0\rangle = 0 \forall \mathbf{k}$. Using Eqs. (1.19) and (1.20), we can obtain the tensor power spectrum as

$$\mathcal{P}_T(k) = 2 \left(\frac{k^3}{2\pi^2} \right) |h_k|^2, \quad (1.21)$$

where the factor of 2 is needed to take into account the two states of polarization, $+$ and \times , of the gravitational waves.

Chapter 2

Inflationary models

As mentioned earlier, neither a matter field nor a radiation field can drive inflation. Therefore, under the necessary conditions, we can assume that a scalar field ϕ and a potential $V(\phi)$ drive inflation. Numerous models for the potential function $V(\phi)$ have been proposed, each capable of driving inflation. Power law inflation, inflation driven by a small field potential model, slow-roll inflation and chaotic inflation are a few such examples. We shall discuss the first two in more detail later in this chapter. The predictions of these models are quantified in terms of the spectral indices of the power spectrum of the scalar and tensor perturbations at super-Hubble scales, namely n_S & n_T and the ratio of tensor to scalar power spectrum at super-Hubble scales r .

In this chapter, we shall look at two models of inflation namely power law inflation and inflation driven by a small field potential model. For the latter of the two models, it is highly non-trivial to solve the background equations analytically. We shall therefore only be able to obtain the analytical solutions for power law inflation. Numerical solutions for the background and the tensor power spectrum for the latter model are discussed in the next chapter. We shall first solve the equations governing the background. Using the solutions of the background equations, we shall solve the equations governing the tensor perturbations and obtain the power spectrum of the tensor perturbations.

From Eq. (1.8), we can write the individual components of the stress-energy tensor for a scalar field ϕ as

$$T_0^0 = \left(\frac{\dot{\phi}^2}{2} \right) + V(\phi) = \rho, \quad (2.1)$$

$$T_j^i = - \left[\left(\frac{\dot{\phi}^2}{2} \right) - V(\phi) \right] \delta_j^i = -p \delta_j^i. \quad (2.2)$$

Using Eqs. (2.1) and (2.2), we can rewrite Eqs. (1.4) and (1.5) as

$$\dot{H} = \frac{-\dot{\phi}^2}{2M_{\text{Pl}}^2}, \quad (2.3)$$

$$H^2 = \left(\frac{1}{3M_{\text{Pl}}^2} \right) \left(\frac{\dot{\phi}^2}{2} + V \right). \quad (2.4)$$

We can now express the scalar field ϕ and the potential V in terms of cosmic time t as

$$\phi(t) = \sqrt{2}M_{\text{Pl}} \int dt \sqrt{-\dot{H}}, \quad (2.5)$$

$$V(t) = M_{\text{Pl}}^2 \left(3H^2 + \dot{H} \right). \quad (2.6)$$

2.1 Power law inflation

Assume that the scale factor has a power-law form during inflation, namely

$$a(t) = a_0 t^q. \quad (2.7)$$

Eq. (2.7) can be written in terms of conformal time η as

$$a(\eta) = (-\bar{\mathcal{H}}\eta)^{(\gamma+1)}, \quad (2.8)$$

where $\bar{\mathcal{H}}$ and γ are given by

$$\bar{\mathcal{H}} = a_0^{1/q}(q-1) \quad \text{and} \quad \gamma = - \left(\frac{2q-1}{q-1} \right). \quad (2.9)$$

We can see that the scalar field and the potential that drive the inflation have the form

$$\frac{\phi(t)}{M_{\text{Pl}}} = \sqrt{(2q)} \ln \left[\sqrt{\left(\frac{V_0}{(3q-1)q} \right)} \left(\frac{t}{M_{\text{Pl}}} \right) \right], \quad (2.10)$$

$$V(\phi) = V_0 \exp \left[-\sqrt{\left(\frac{2}{q} \right)} \left(\frac{\phi}{M_{\text{Pl}}} \right) \right]. \quad (2.11)$$

In terms of e-fold N , we can rewrite $\phi(t)$ as

$$\frac{\phi(N)}{M_{\text{Pl}}} = \sqrt{\left(\frac{2}{q} \right)} N - \sqrt{(2q)} \ln t_0. \quad (2.12)$$

where $t_0 = \sqrt{((3q-1)q/V_0)}$

Similarly, we can write the Hubble parameter H in terms of e-fold N as

$$H(N) = H_0 \exp^{-N/q}. \quad (2.13)$$

We also introduce a new parameter $\epsilon_1(N)$, which is defined as

$$\epsilon_1(N) = \frac{1}{2} \left(\frac{d\phi}{dN} \right)^2 = \frac{1}{q}, \quad (2.14)$$

Having solved for the scalar field and the Hubble parameter, we can now attempt to solve the equation governing the tensor perturbations. We can rewrite Eq. (1.16), by substituting $h_k = (u_k/a)$, as

$$u_k'' + \left[k^2 - \left(\frac{a''}{a} \right) \right] u_k = 0, \quad (2.15)$$

and the power spectrum governing tensor perturbations, namely Eq. (1.21), becomes

$$\mathcal{P}_T(k) = 2 \left(\frac{k^3}{2\pi^2} \right) |h_k|^2 = 2 \left(\frac{k^3}{2\pi^2} \right) \left(\frac{|u_k|}{a} \right)^2. \quad (2.16)$$

2.1.1 The Bunch-Davies initial conditions

In order to arrive at the analytical solutions to the tensor perturbations in fourier space, we need to understand the initial conditions from which these perturbations evolved. We impose the initial conditions when the modes are well inside the Hubble radius i.e when $\eta \rightarrow -\infty$ or $(k/aH) \gg 1$. In such a sub-Hubble limit, the curvature of spacetime can be neglected. Further, upon imposing the condition that u_k are positive frequency modes, we can arrive at the solution to the Eq. (2.15) in the sub-Hubble limit as

$$\lim_{(k/aH) \rightarrow \infty} u_k(\eta) \rightarrow \left(\frac{1}{\sqrt{2k}} \right) e^{-ik\eta}. \quad (2.17)$$

2.1.2 Tensor power spectrum

Now that we've obtained the solutions for the background and the initial conditions governing the tensor perturbations, we shall attempt to solve the equation governing the tensor perturbations and obtain the power spectrum of the tensor perturbations.

Substituting the scale factor given by Eq. (2.7) in the Eq. (2.15), we can arrive at a solution that satisfies the initial conditions Eq. (2.17) as

$$u_k(\eta) = \left(\frac{-\pi\eta}{4} \right)^{1/2} e^{i[\nu+(1/2)](\pi/2)} H_\nu^{(1)}(-k\eta), \quad (2.18)$$

where $\nu = [\gamma + (1/2)]$ and $H_\nu^{(1)}$ is the Hankel function of the first kind and of order ν (Ref. [11]).

In the super-Hubble limit (i.e as $(-k\eta \rightarrow 0)$), we can approximate the Hankel function to

$$H_\nu^{(1)}(z) \sim -(i/\pi)\Gamma(\nu) \left(\frac{z}{2} \right)^{(-\nu)}. \quad (2.19)$$

where $\Gamma(\nu)$ is a Gamma function.

In the super-Hubble limit, u_k and the scale factor a have similar behaviour. Therefore, the tensor amplitude h_k reaches a constant value and the tensor power spectrum can be written as

$$\mathcal{P}_T(k) = A_T \bar{\mathcal{H}}^2 \left(\frac{k}{\bar{\mathcal{H}}} \right)^{2(\gamma+2)}, \quad (2.20)$$

where

$$A_T = \left[\frac{1}{\pi^3 M_{\text{Pl}}^2} \right] \left(\frac{|\Gamma(\nu)|^2}{2^{(2\gamma+1)}} \right). \quad (2.21)$$

In this case, the spectral index of the tensor power spectrum in the super-Hubble limit is

$$n_T = 2(\gamma + 2) = \frac{-2}{q - 1}. \quad (2.22)$$

2.2 Inflation driven by small field potential

We shall assume that the potential $V(\phi)$ that drives inflation is of the form

$$V = V_0 \left[1 - \left(\frac{\phi}{\mu} \right)^p \right], \quad (2.23)$$

where $p = 4$, $\mu/M_{\text{Pl}} = 15$ and $V_0/M_{\text{Pl}}^4 = 5.55702 \times 10^{-10}$.

Substituting Eq. (2.23) in Eq. (1.9) and using the expression for H from the Eq. (2.4), we get

$$\ddot{\phi} + \left(\frac{\sqrt{3}}{M_{\text{Pl}}} \right) \left(\frac{\dot{\phi}^2}{2} + V \right) \dot{\phi} - \frac{pV_0}{\mu} \left(\frac{\phi}{\mu} \right)^{(p-1)} = 0. \quad (2.24)$$

We shall not attempt to obtain an analytical solution for the above expression, instead we solved for $\phi(N)$ numerically. Further details regarding the numerical procedure are provided in the next chapter.

Chapter 3

Numerical results

In this section, I describe the procedure adopted to numerically evaluate the tensor power spectrum of gravitational waves in a power-law inflationary scenario and in a scenario where inflation is driven by a small-field potential model. Note that we are working in units of $M_{\text{Pl}} = 1$.

3.1 Power-law inflation

Assuming an inflationary potential $V(\phi)$ of the form

$$V(\phi) = V_0 \exp \left[-\sqrt{\frac{2}{q}} (\phi - \phi_i) \right], \quad (3.1)$$

where ϕ represents the scalar field driving inflation, ϕ_i is the initial value at $N = 0$ and q is the power-law index.

Eqn (1.9) can be written in terms of e-fold time N as

$$\frac{d^2\phi}{dN^2} + \left[3 - \frac{1}{2} \left(\frac{d\phi}{dN} \right)^2 \right] \frac{d\phi}{dN} + \left[6 - \left(\frac{d\phi}{dN} \right)^2 \right] \frac{1}{2V(\phi)} \frac{dV(\phi)}{dN} = 0. \quad (3.2)$$

Note that I have made use of the following definition for H to arrive at the above expression

$$H^2 = \frac{2V(\phi)}{3 - (d\phi/dN)^2}. \quad (3.3)$$

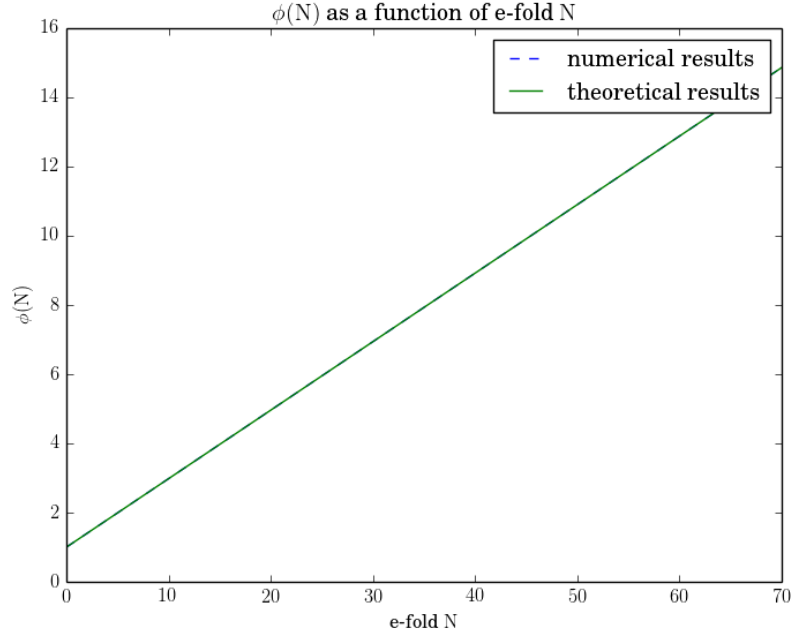


Figure 3.1: Plot of $\phi(N)$ as a function of N during power law inflation

We numerically integrate the Eq.(3.2) using a fourth-order Runge-Kutta method, implemented in Python (Refs. [12, 13, 14]). Integration was performed from e-fold time $N = 0$ to $N = 70$ while assuming the initial conditions for ϕ and $d\phi/dN$ at $N = 0$ to be

$$\frac{\phi}{M_{\text{Pl}}} = 1, \quad (3.4)$$

and

$$\frac{d\phi}{dN} = \left(\frac{\sqrt{2q}}{t_0} \frac{1}{H_0} \right) M_{\text{Pl}}, \quad (3.5)$$

where H_0 is the value of the Hubble parameter at $N = 0$.

Figures 3.1, 3.2 and 3.3 show the theoretical and numerical estimate of ϕ , H and ϵ_1 as a function of N . As can be seen, the theoretical and numerical estimates are in good agreement with one another.

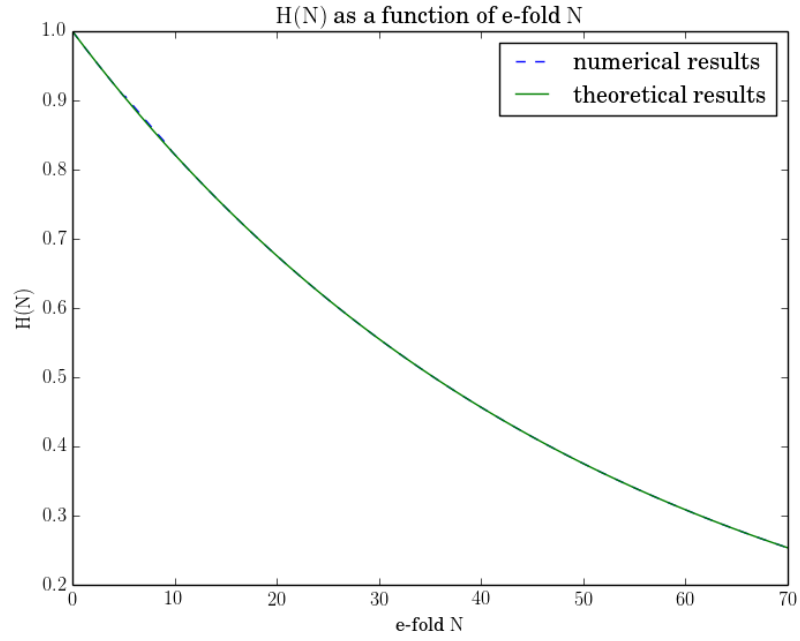


Figure 3.2: Plot of $H(N)$ as a function of N during power law inflation

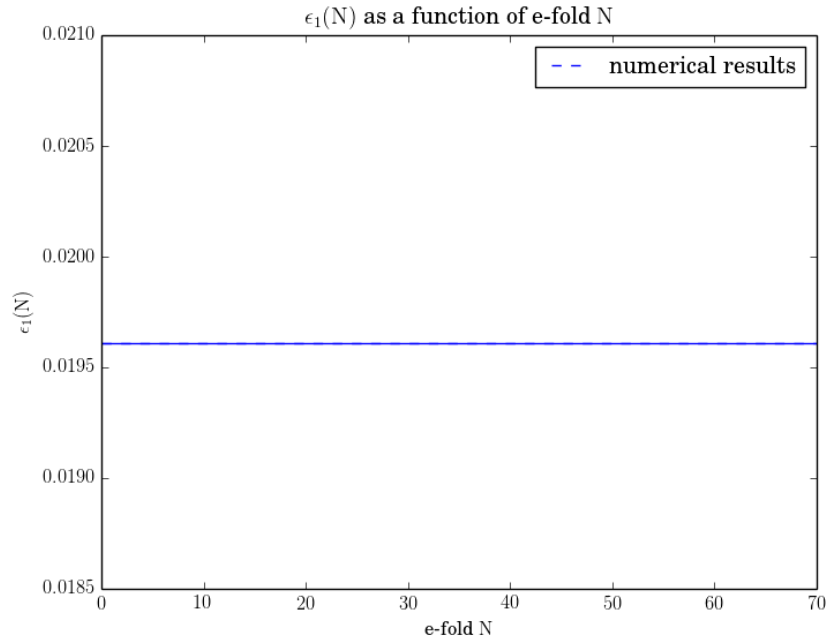


Figure 3.3: Plot of $\epsilon_1(N)$ as a function of N during power law inflation

Using the numerical solutions to the background, namely $\phi(N)$ and $H(N)$, we can now solve the equation governing the tensor perturbations. Rewriting the Eq. (1.18) in terms of e-fold time, we arrive at

$$\frac{d^2 h_k}{dN^2} + \left(3 + \frac{1}{H} \frac{dH}{dN} \right) \frac{dh_k}{dN} + \frac{k^2}{a^2 H^2} h_k = 0. \quad (3.6)$$

The above equation was numerically integrated using a fourth order Runge-Kutta method, implemented in Python. It is to be noted that h_k was numerically evaluated for various values of k , ranging from 10^{-6} to 10^0 Mpc^{-1} . For each value of k , the initial and final limits of integration in terms of e-fold N were calculated by solving for N when the modes are well inside the Hubble scale ($k/aH = 100$) and when the modes are well outside the Hubble scale ($k/aH = 10^{-5}$). Using Eq. (2.17), the initial values for h_k and dh_k/dN were set to be

$$h_k = \frac{1}{\sqrt{2k_0} a(N)}, \quad (3.7)$$

$$\frac{dh_k}{dN} = -\frac{1}{\sqrt{2k_0} a(N)} - \frac{i\sqrt{(k_0/2)}}{a^2(N)H(N)}, \quad (3.8)$$

Now that we have successfully obtained a numerical solution for h_k , we can evaluate the tensor power spectrum using Eq. (1.21). Figure 3.4 shows the numerical estimate of $\mathcal{P}_T(k)$ as a function of k .

3.2 Inflation driven by a small field potential

For a small field potential model, given by Eq. (2.23), we repeated the above process to estimate the scalar field ϕ , the Hubble parameter H , ϵ_1 and the tensor power spectrum $\mathcal{P}_T(k)$.

To solve the background equation governing the evolution of ϕ numerically, we assumed that at $N = 0$, $\phi/M_{\text{Pl}} = 7.3$ and that $\dot{\phi}/M_{\text{Pl}}^2 = 8 \times 10^{-7}$.

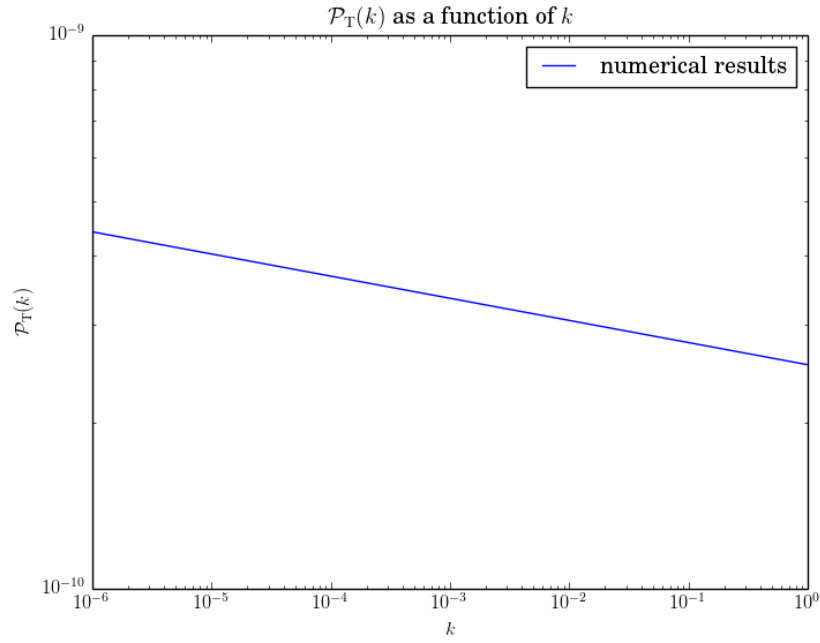


Figure 3.4: Plot of $\mathcal{P}_T(k)$ as a function of k during power law inflation

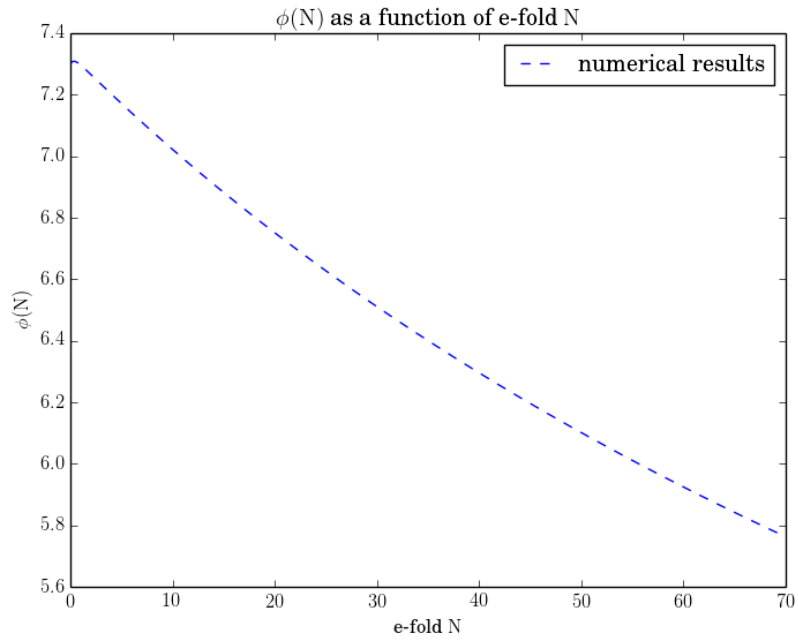


Figure 3.5: Plot of $\phi(N)$ as a function of N during inflation driven by a small field potential

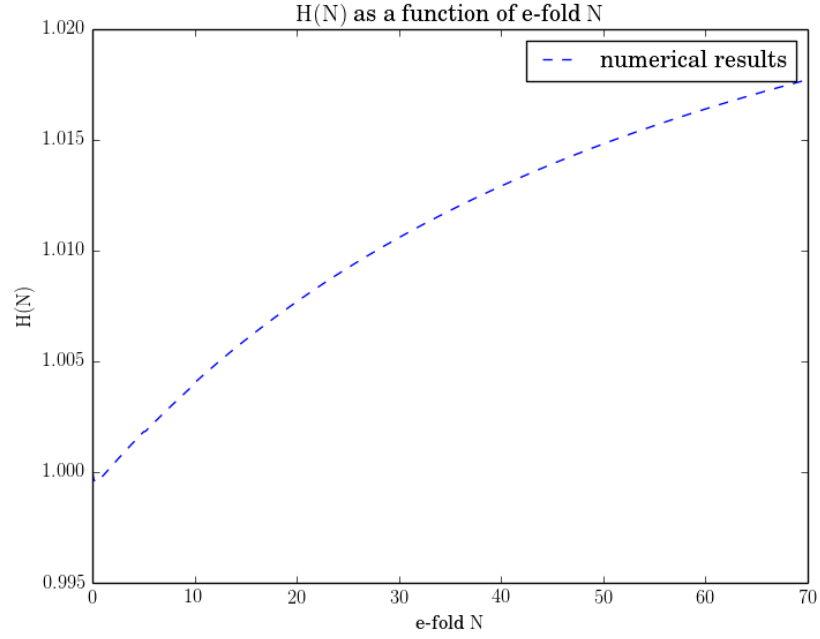


Figure 3.6: Plot of $H(N)$ as a function of N during inflation driven by a small field potential

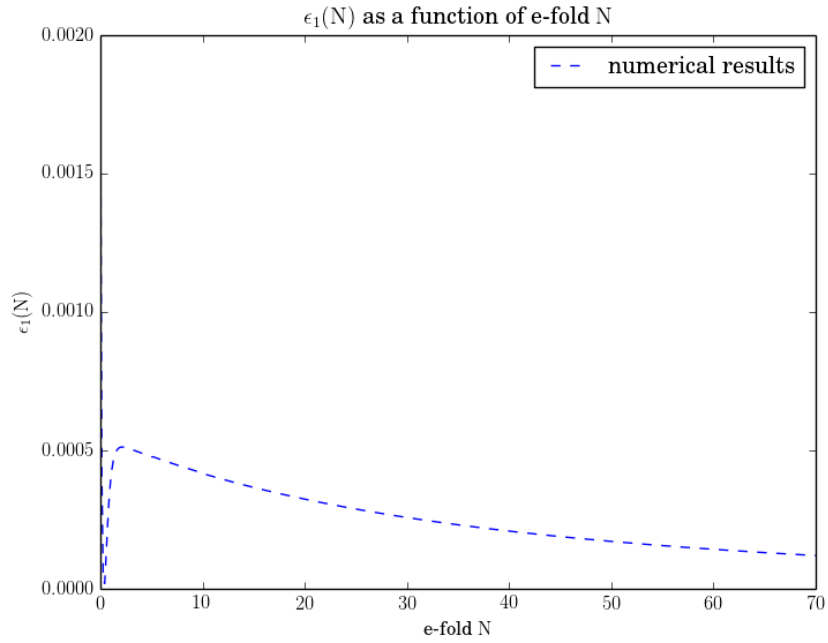


Figure 3.7: Plot of $\epsilon_1(N)$ as a function of N during inflation driven by a small field potential

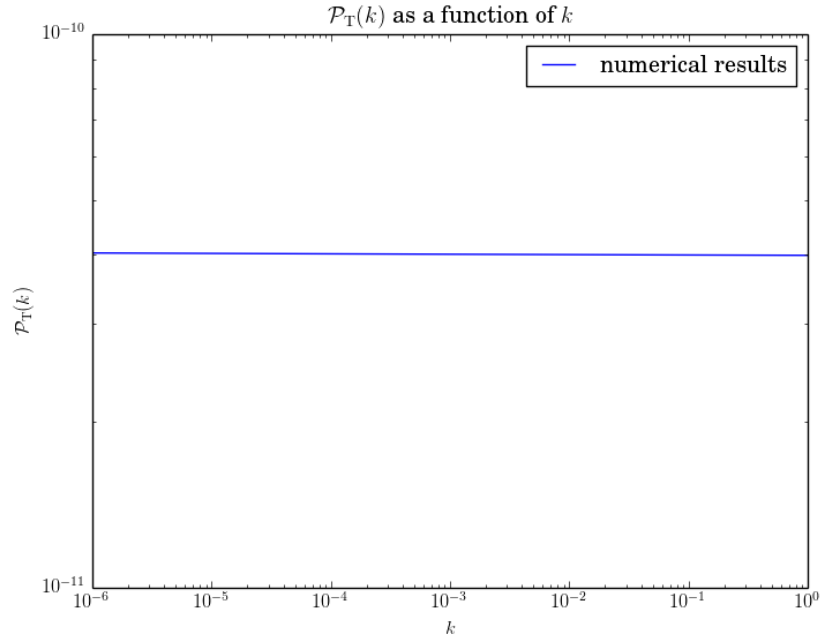


Figure 3.8: Plot of $\mathcal{P}_T(k)$ as a function of k during inflation driven by a small field potential

Figures 3.5, 3.6 and 3.7 show the numerical estimates of ϕ , H and ϵ_1 as a function of N . Figure 3.8 shows the numerical estimate of the tensor power spectrum $\mathcal{P}_T(k)$ as a function of k during inflation driven by small field model of potential.

Chapter 4

Summary

In this thesis, we have studied tensor perturbations in the metric and evaluated the power spectrum of the tensor perturbations. We have also numerically estimated the power spectrum of tensor perturbations in the super-Hubble limit.

In the first chapter, we discussed how neither a matter field nor a radiation field can drive inflation and we understood the conditions imposed on a scalar field to drive inflation. We had written down the stress-energy tensor corresponding to the scalar field and we arrived at the equation governing the evolution of the scalar field. Using the perturbed Einstein tensors and the perturbed stress-energy tensor, we were able to arrive at an equation governing the evolution of tensor perturbations. We then quantized the tensor perturbations in terms of it's Fourier modes and arrived at an analytic form of the power spectrum of tensor perturbations.

In the second chapter, we discussed the analytical solutions of the scalar field ϕ and the potential $V(\phi)$ during power law inflation. After solving the background, we obtained an analytic solution to the tensor perturbations and obtained the power spectrum of tensor perturbations in the super-Hubble limit. We briefly discuss inflation driven by a small field potential model.

In the third chapter, we discussed the methods used to arrive at the numerical solutions to the scalar field, the Hubble parameter and ϵ_1 as a function of e-fold N and the tensor power spectrum $\mathcal{P}_T(k)$ as a function of k . We studied two forms of the potential, namely

power law and small field models of the potential. Using a python code, we were able to obtain numerical solutions that were in good agreement with the theoretical estimates for power law inflation. We also arrived at the numerical solutions for the small field potential model.

Bibliography

- [1] L. Sriramkumar, arXiv:0904.4584.
- [2] S. Dodelson, *Modern Cosmology* (Academic Press, San Diego, 2003).
- [3] R. Durrer, *Fund. Cosmic Phys.* **15**, 209 (1994).
- [4] A. Riotto, arXiv:hep-ph/0210162.
- [5] W. H. Kinney, astro-ph/0301448.
- [6] A. D. Linde, *Particle Physics and Inflationary Cosmology* (Harwood Academic, Switzerland, 1990).
- [7] R. H. Brandenberger, *Rev. Mod. Phys.* **1**, 57 (1985).
- [8] V. F. Mukhanov, H. A. Feldman, and R. H. Brandenberger, *Phys. Rep.* **215**, 203 (1992).
- [9] M. Giovannini, *Int. J. Mod. Phys. D* **14**, 363 (2005).
- [10] A. Guth, *Phys. Rev. D* **23**, 347 (1981).
- [11] M. Abramowitz and I. A. Stegun, *Handbook of Mathematical Functions* (Dover Publications, New York, 1964).
- [12] Guido van Rossum: *Python Reference Manual*, CWI Report CS-R9525 (1995).
- [13] Stefan van der Walt, S. Chris Colbert and Gael Varoquaux, *Computing in Science and Engineering* **13**, 22 (2011).
- [14] John D. Hunter, *Computing in Science and Engineering* **9**, 90 (2007).

Appendix A

Python Code

We have attached a python code that evaluates the theoretical and numerical estimates for the scalar field ϕ , the Hubble parameter H , ϵ_1 as a function of e-fold N and the power spectrum of the tensor perturbations in the super-Hubble limit $\mathcal{P}_T(k)$ as a function of k during power law inflation. To arrive at the numerical estimates during inflation driven by a small field potential model, we shall replace the potential function with Eq. (2.23) and change the relevant constants.

Eq. (3.2) is solved numerically using a fourth order Runge-Kutta method and H , ϵ_1 are obtained from the numerical solution of $\phi(N)$. After we solve the background, we solve Eq. (3.6) numerically using a fourth order Runge-Kutta method. Using the numerical solutions for h_k and Eq. (1.21), we can numerically evaluate the power spectrum. Note that we are working in units of $M_{\text{Pl}} = 1$

```

import numpy
import matplotlib.pyplot as plt

plt.rc('text', usetex=True)
plt.rc('font', family='serif')

tps_file = open('power_spectrum_power_law.dat','w')
phi_file = open('phi_vs_N_power_law.dat','w')
h_file = open('H_vs_N_power_law.dat','w')
eps_file = open('eps1_vs_N_power_law.dat','w')

q = 51.
V0 = (204./100.)*1e-08
t0 = (q*(3.*q -1.)/V0)**(1./2)

phi0 = 1.
dphi0 = (2.*q)**(1./2)/t0

Ni = 0.
Nf = 70.

kp = 5.*1e-02
beta = -((2.*q -1.)/(q -1.))
eps1a = ((beta +2.)/(beta +1.))

V = lambda phi : V0*numpy.exp(-(2./q)**(1./2)*(phi -phi0))
dV=lambda phi :-(2./q)**(1./2)*V0*numpy.exp(-(2./q)**(1./2)*(phi -phi0))

H0 = ((1./3)*(dphi0**2/2. +V(phi0)))*(1./2.)
Dphi0 = dphi0/H0

def DDphi(N, phi0, Dphi0):
    return -(3 -Dphi0**2/2.)*Dphi0 -(dV(phi0)/(2*V(phi0)))*(6 -Dphi0**2)

def rk4_step(N, phi0, Dphi0, step):
    F1 = Dphi0
    f1 = DDphi(N, phi0, Dphi0)
    F2 = Dphi0 +f1*step/2.
    f2 = DDphi(N +step/2., phi0 +F1*step/2., Dphi0 +f1*step/2.)
    F3 = Dphi0 +f2*step/2.
    f3 = DDphi(N +step/2., phi0 +F2*step/2., Dphi0 +f2*step/2.)
    F4 = Dphi0 +f3*step
    f4 = DDphi(N +step, phi0 +F3*step, Dphi0 +f3*step)

    return [(f1 +2*f2 +2*f3 +f4)*step/6.,
            (F1 +2*F2 +2*F3 +F4)*step/6.] # [Dphi, phi] update

```

```

npts = 100000
step = (Nf-Ni)/(npts)

phi_ = phi0
Dphi_ = Dphi0

phi_array = numpy.array([phi_])
Dphi_array = numpy.array([Dphi_])
N_array = numpy.array([Ni])

phi_theory = lambda N : (2./q)**(1./2)*N + phi0

N = Ni
phi_file.write(str(N)+"\t"+str(phi_)+"\t"
+str(Dphi_)+"\t"+str(phi_theory(N))+"\n")
while N < Nf:
    array = rk4_step(N, phi_, Dphi_, step)
    phi_ = phi_ + array[1]
    Dphi_ = Dphi_ + array[0]
    phi_array = numpy.append(phi_array,phi_)
    Dphi_array = numpy.append(Dphi_array,Dphi_)
    N += step
    N_array = numpy.append(N_array,N)
    phi_file.write(str(N)+"\t"+str(phi_)+"\t"
+str(Dphi_)+"\t"+str(phi_theory(N))+"\n")

phi_file.close()

phi = lambda N : phi_array[int((N-Ni)/step)]
Dphi = lambda N : Dphi_array[int((N-Ni)/step)]

plt.cla()
plt.hold(True)
plt.xlim([Ni,Nf])
plt.xlabel(r'e-fold  $\{\rm N\}$ ')
plt.ylabel(r' $\phi(\{\rm N\})$ ')
plt.title(r' $\phi(\{\rm N\})$  as a function of e-fold  $\{\rm N\}$ ')
numerical, = plt.plot(N_array, phi_array,
'--', label = 'numerical results')
theory, = plt.plot(N_array, [phi_theory(N) for N in N_array],
'-', label = 'theory results')
plt.legend([numerical, theory],
['numerical results', 'theoretical results'])
plt.savefig('phi_vs_N_power_law.png')

```

```

eps0 = (3./2)*((dphi0**2)/(dphi0**2/2. + V(phi0)))
eps = 1./q

H = lambda N : (V(phi(N))/(3 -Dphi(N)**2/2))**(1./2)
DH = lambda N : H(N)*Dphi(N)

H_theory = lambda N : H0*numpy.exp(-N/q)

for N in N_array:
h_file.write(str(N)+"\t"+str(H(N)/H0)+"\t"+str(H_theory(N)/H0)+"\n")

plt.cla()
plt.hold(True)
plt.xlim([Ni,Nf])
plt.xlabel(r'e-fold  $\{\rm N\}$ ')
plt.ylabel(r' $\{\rm H\}(\{\rm N\})$ ')
plt.title(r' $\{\rm H\}(\{\rm N\})$  as a function of e-fold  $\{\rm N\}$ ')
numerical, = plt.plot(N_array, numpy.asarray([H(i) for i in N_array],
dtype= numpy.float64)/H0, '--', label = 'numerical results')
theory, = plt.plot(N_array, [H_theory(N)/H0 for N in N_array],
'--', label = 'theory')
plt.legend([numerical, theory],
['numerical results', 'theoretical results'])
plt.savefig('H_vs_N_power_law.png')

ai = 1e-05

eps1 = lambda N : Dphi_array[int((N-Ni)/step)]**2/2.
eps1_theory = eps0

for N in N_array:
eps_file.write(str(N)+"\t"+str(eps1(N))+"\t"+str(eps1_theory)+"\n")

plt.cla()
plt.xlim([Ni,Nf])
plt.xlabel(r'e-fold  $\{\rm N\}$ ')
plt.ylabel(r' $\{\rm \epsilon_1\}(\{\rm N\})$ ')
plt.title(r' $\{\rm \epsilon_1\}(\{\rm N\})$  as a function of e-fold  $\{\rm N\}$ ')
numerical, = plt.plot(N_array,
[str(eps1(i)).strip('[]') for i in N_array],
'--', label = 'numerical results')
plt.axhline(y=eps0)
plt.legend([numerical], ['numerical results'])
plt.savefig('eps1_vs_N_power_law.png')

z = lambda N: ai*numpy.exp(N)*Dphi(N)

```

```

A = lambda N : ai*numpy.exp(N)

def DDhk(k0, N, hk0, Dhk0):
    return -((3. + (DH(N)/H(N)))*Dhk0 + ((k0/(A(N)*H(N)))**2)*hk0)

def rk4_step(k0, N, hk0, Dhk0, step):
    F1 = Dhk0
    f1 = DDhk(k0, N, hk0, Dhk0)
    F2 = Dhk0 + f1*step/2.
    f2 = DDhk(k0, N + step/2., hk0 + F1*step/2., Dhk0 + f1*step/2.)
    F3 = Dhk0 + f2*step/2.
    f3 = DDhk(k0, N + step/2., hk0 + F2*step/2., Dhk0 + f2*step/2.)
    F4 = Dhk0 + f3*step
    f4 = DDhk(k0, N + step, hk0 + F3*step, Dhk0 + f3*step)

    return numpy.array([(f1 + 2*f2 + 2*f3 + f4)*step/6.], dtype=complex),
           numpy.array([(F1 + 2*F2 + 2*F3 + F4)*step/6.], dtype=complex)
    # [Dhk, hk] update

k_list = numpy.array([10**((-12 + i)/2.) for i in range(13)])
Nics_array = []
Nshs_array = []

for k in k_list:
    Nics_temp = numpy.asarray([k - 1e+02*A(N)*H(N) for N in N_array])
    Nshss_temp = numpy.asarray([k - 1e-05*A(N)*H(N) for N in N_array])
    nics_test = numpy.where(Nics_temp > 0)
    nshss_test = numpy.where(Nshss_temp > 0)
    Nics_array.append(Ni + nics_test[0][-1]*step)
    Nshs_array.append(Ni + nshss_test[0][-1]*step)

Nics_arr = numpy.asarray(Nics_array)
Nshs_arr = numpy.asarray(Nshs_array)

k_min = 1e-6
k_max = 10**(1./2)

k_vs_hk = numpy.zeros(1, dtype=complex)

i = 0
k0 = k_min

while k0 < k_max:
    print 'k0 = ', k0

    Nics = Nics_arr[i]

```

```

Nshss = Nshs_arr[i]

hk0 = numpy.zeros(1, dtype=complex)
hk0.real = ((2.*k0)**(1./2))*A(Nics)**(-1.)

Dhk0 = numpy.zeros(1, dtype=complex)
Dhk0.real = -(1/A(Nics))*((2*k0)**(-1./2))
Dhk0.imag = -((k0/2)**(1./2))/(A(Nics)*A(Nics)*H(Nics))

N = Nics
while N < Nshss:
    array = rk4_step(k0, N, hk0, Dhk0, step)
    hk0 = hk0 + array[1]
    Dhk0 = Dhk0 + array[0]
    N += step

k_vs_hk = numpy.append(k_vs_hk, hk0)
print '\n'

temp = 8*(k0)**3/(2*numpy.pi**2)*(numpy.absolute(hk0))**2
tps_file.write(str(k0)+"\t"+str(temp).strip('[]')+"\n")
k0 = 10**(1./2)*k0
i += 1

k_list = numpy.array([10**((-12 + i)/2.) for i in range(13)])
TPS = [8*(k_list[i])**3/(2*numpy.pi**2)*
(numpy.absolute(k_vs_hk[i+1]))**2 for i in range(len(k_list))]
print k_list, TPS

tps_file.close()

plt.cla()
plt.xlabel(r'$k$')
plt.ylabel(r'$\mathcal{P}_{\rm T}(k)$')
plt.title(r'$\mathcal{P}_{\rm T}(k)$ as a function of $k$')
numerics, = plt.loglog(k_list, TPS)
plt.legend([numerics], ['numerical results'])
plt.savefig('power_spectrum_power_law.png')

```